

Supplementary Information

Structural Analysis of Healthy and Cancerous Epithelial Breast Type Cells by Nanomechanical Spectroscopy Allows to Obtain Peculiarities of Skeleton and Junctions

Anahid Amiri,^{*a}, Florian Hastert,^b Lukas Stühn,^a and Christian Dietz^{*a}

^aPhysics of Surfaces, Institute of Materials Science, Technische Universität Darmstadt, Alarich-Weiss-Str. 2, 64287 Darmstadt, Germany

^bCell Biology and Epigenetics, Department of Biology, Technische Universität Darmstadt, 64287 Darmstadt, Germany

*Email: anahid.amiri@stud.tu-darmstadt.de, dietz@pos.tu-darmstadt.de

Stiffness of substructures of ductal epithelial healthy and cancerous breast type cell lines

The presence of ions as well as positively and negatively charged molecules in the cell is necessary for some cellular processes to occur for instance proteins transportation into or out of the cell. The silicon nitride cantilever is positively charged in slightly acidic CO₂-independent medium with a pH value ≈ 6.5 , which was used for measuring cells *in situ*.¹ The effect of positive and negative charges as well as mechanical forces on the tip attached to a very soft cantilever inside the cell structure can be impressively seen in the force vs. indentation graphs of Figure S1 (left column). Moreover, the effective stiffness as derivate of the force as function of the indentation is depicted in the right column of Figure S1. The electrostatic

interaction between tip and cells' components was sufficiently high to cause an initially negative deflection of the cantilever. For the sake of deriving the tip indentation, we subtracted the cantilever deflection values from respective z -piezo positions which resulted in an initial indentation at zero z position of the piezo in each cantilever oscillation cycle. When the cantilever was located on membrane protected structures, the initial indentation showed values between 20 – 30 nm on microtubules (Figure S1a) and 10 – 20 nm on intermediate filaments (Figure S1e). By considering the membrane thickness that is approx. 10 nm,² based on the initial engagement and the fact that we do not see any attachment/detachment events in the force vs. indentation cycles, we concluded that the tip did not leave the cell during the measurement of the cells' inner substructures. In case of microtubules and intermediate filaments which are placed in elevated positions compared to the nucleus and actin network but underneath the cell membrane, we can interpret the peak in stiffness derived on each of the substructure as their initial stiffness sensed by the tip individually, without concerning about membrane stiffness on top of them (graphs in Figs S1b and S1f). We know that the actin network is placed near the substrate, hence we considered the plateau value sensed at higher indentation (approx. 300 nm) force derivative vs. indentation graph as stiffness value for F-actin (Figure S2b). Comparing filaments stiffness calculated as force derivative with respect to indentation illustrates microtubules as the most rigid filaments sensed by the tip among all three. For microtubules, densely sensed in HBL100, the average stiffness was 250 pN/nm and for intermediate filaments in both cell types was approximately 140 pN/nm. Due the flexibility of the BT20 cell line, the tip could penetrate completely through the cell structure and consequently actin filaments could be only sensed in BT20 cells with the force setpoint value that was used. Their corresponding stiffness revealed very low values of 10 pN/nm at maximum. The low value found on these structures could arise mainly from the positively charged silicon nitride tip and the plasma treated substrate causing OH⁻ groups at its surface leading to an overall negative charge where the proximity of the tip to the substrate leads to high attractive interactions and dominates the

overall forces sensed by the tip. Approximate absence of MTs as one of the most rigid filaments of eukaryotic cell in IDCs could highly justify the larger deformability and softness in cancerous cells in comparison to their counterparts.

In addition to the stiffness of cell cytoskeleton components which has been sensed by the cantilever tip, we could extract the stiffness values of epithelial cells junctions such as adherens junction which was approximately 113 pN/nm (Figure S1d) in healthy mammary cells and around 26 pN/nm in IDCs (Figure S2d). Furthermore, the desmosomes junction stiffness in healthy cells was approximately 20 pN/nm (Figure S1d) and in cancerous the stiffness was approximately 35 pN/nm (Figure S2d). Further details we could observe about the characteristics of these junctions on both cell lines are discussed in the main article.

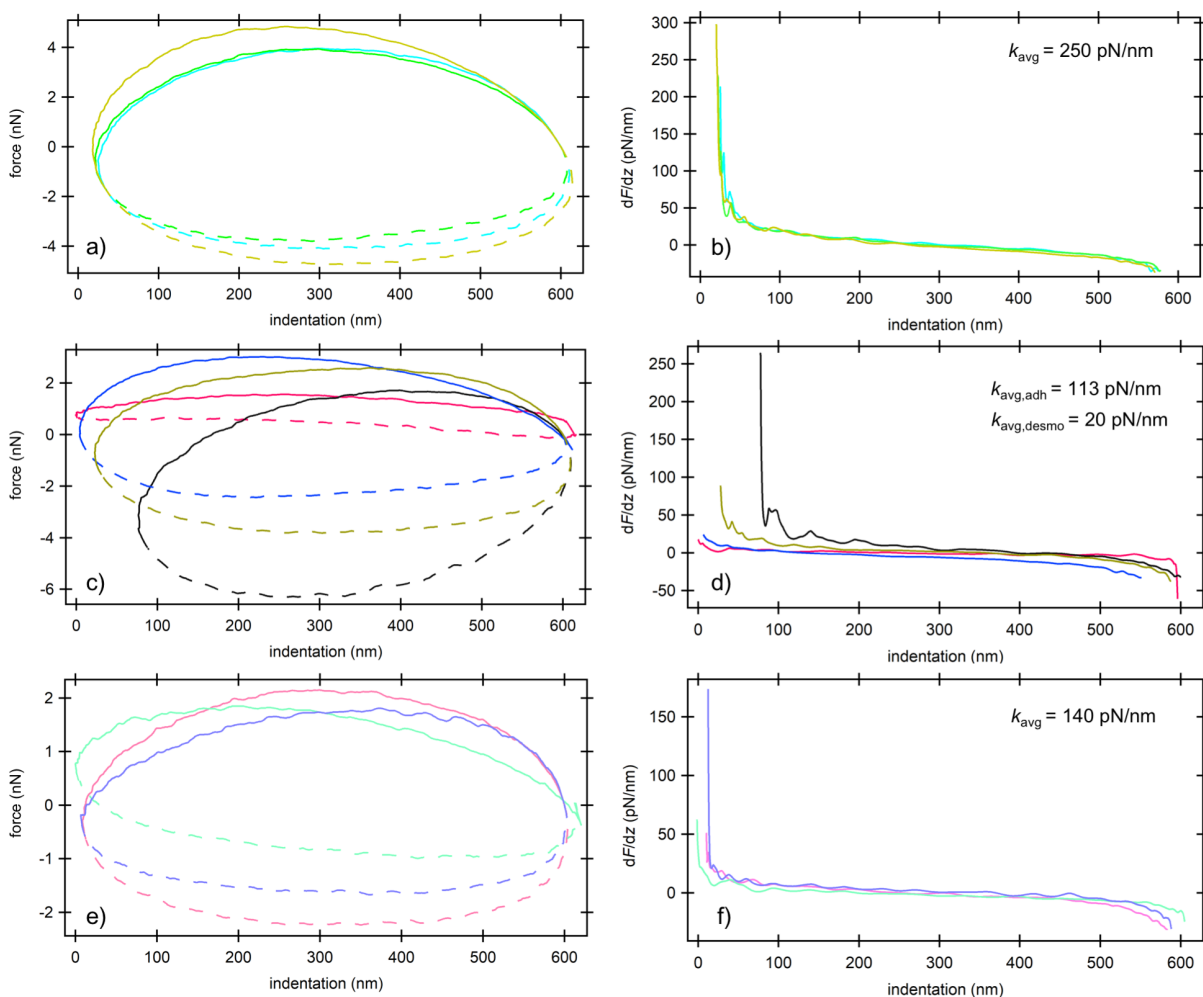


Fig. S1 Atomic force microscopy spectroscopy results on healthy mammary cells (HBL-100). Force vs. indentation curves measured on a, microtubules, c, adherens (black, gold and blue) and desmosomes (dark pink) junctions and e, intermediate filaments. b, Effective stiffness values deduced from the derivative of the force with respect to the indentation for b, microtubules, d, adherence (black, gold, blue) and desmosomes (dark pink) junctions and f, intermediate filaments. Solid lines are to the trace portion of the oscillation cycle whereas the dashed lines are the retrace portions. The color of the curves correspond to the color of the arrows in Figure 3a pointing out the location where the spectroscopy data was extracted.

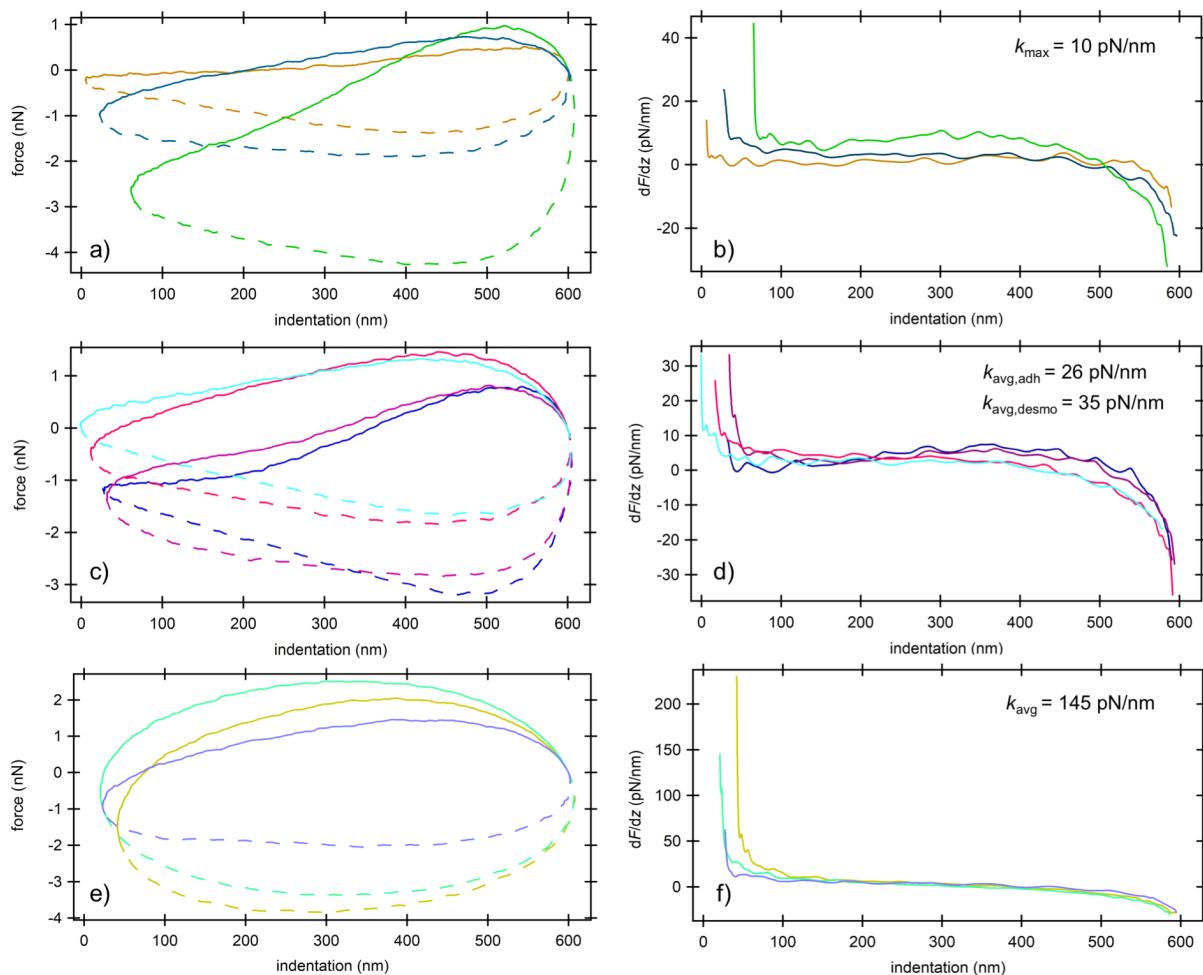


Fig. S2 Atomic force microscopy spectroscopy results on invasive ductal carcinoma cells (BT-20). Force vs. indentation curves measured on a, F-actin, c, adherens (purple, pink and dark blue) and desmosomes (turquoise) junctions and e, intermediate filaments. b, Effective stiffness

values deduced from the derivative of the force with respect to the indentation for b, F-actin, d, adherence (purple, pink and dark blue) and desmosomes (turquoise) junctions and f, intermediate filaments. Solid lines are to the trace portion of the oscillation cycle whereas the dashed lines are the retrace portions. The color of the curves correspond to the color of the arrows in Figure 1b pointing out the location where the spectroscopy data was extracted.

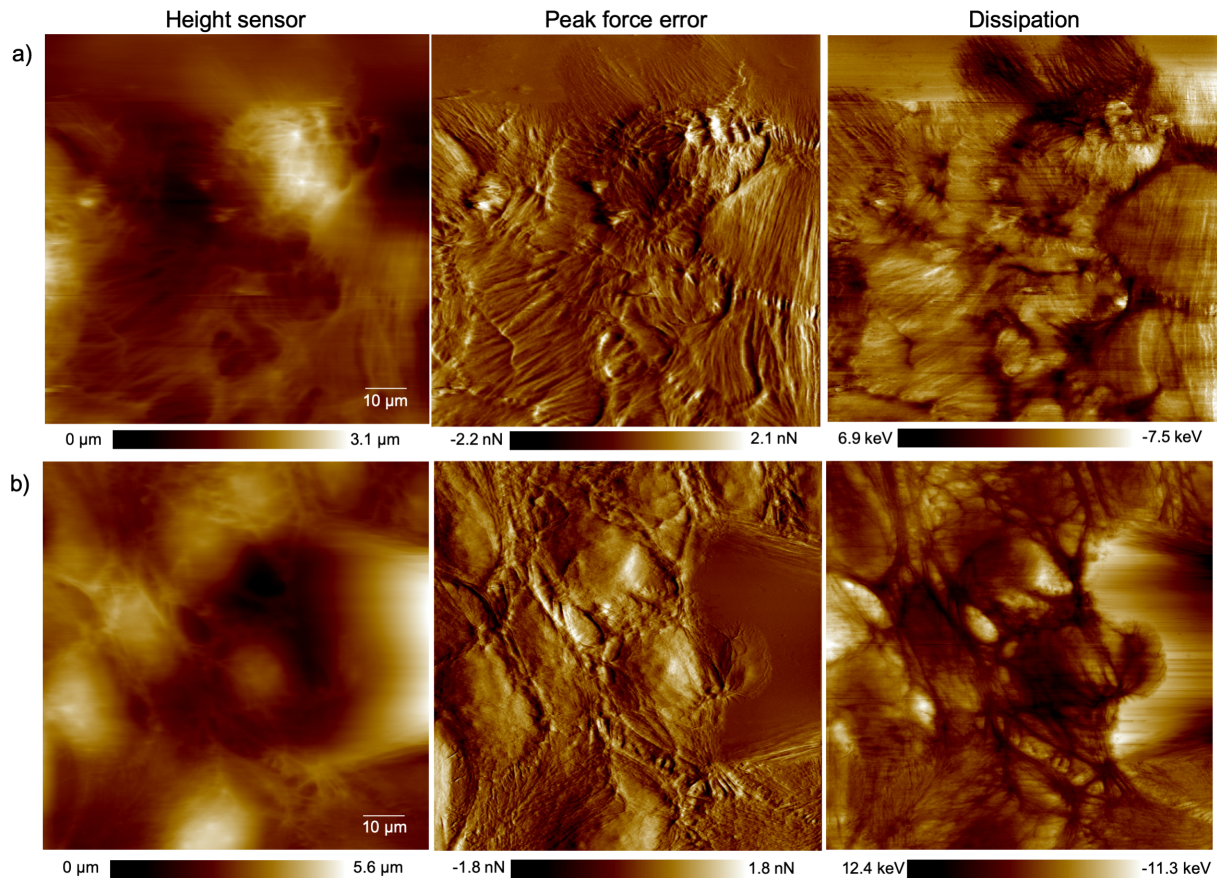


Fig. S3 High resolution topography, force error and dissipation maps of (a) healthy mammary and (b) invasive ductal carcinoma cells.

Table S1 Cell size and shape quantification based on the dimensions taken from the dissipation images in Figs. 1b and 4a.

| Type | HBL100 | | | BT20 | | |
|----------|--------------------------|-------------------------|-------|--------------------------|-------------------------|-------|
| Cell Nr. | Length [μm] | Width [μm] | ratio | Length [μm] | Width [μm] | ratio |
| 1 | 29.5 | 20.3 | 1.5 | 29.0 | 20.0 | 1.5 |
| 2 | 33.5 | 20.5 | 1.6 | 31.7 | 26.4 | 1.2 |
| 3 | 26.7 | 16.0 | 1.7 | 32.1 | 25.5 | 1.3 |
| Average | 29.9 | 18.9 | 1.6 | 30.9 | 24.0 | 1.3 |

To demonstrate the influence of the driving frequency on the shape of the force vs. distance curve a curve captured on BT-20 cell nucleus with a slow drive frequency of 20 Hz is shown in Fig. S3.

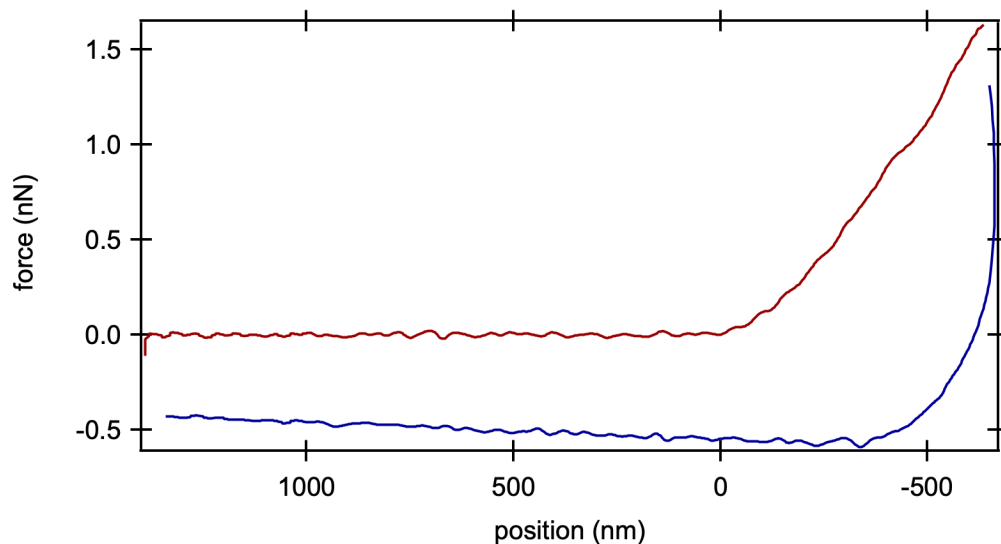


Fig. S4 Force vs. z-piezo position measured on the nucleus region of a BT20 cell using a standard force spectroscopy with a driving frequency of 20 Hz.

References

- 1 J. Biscan, N. Kallay and T. Smolic, *Colloids and Surfaces a-Physicochemical and Engineering Aspects*, 2000, **165**, 115-123.
- 2 M. L. Rodriguez, P. J. McGarry and N. J. Sniadecki, *Appl. Mech. Rev.*, 2013, **65**, 41.